Using General Relativity to Understand Neutron Stars

Sharon Morsink

Department of Physics, University of Alberta, Edmonton, Canada

THE NICER LIGHTCURVE MODELING WORKING GROUP

Slavko Bogdanov (chair), Zaven Arzoumanian, Keith Gendreau, Anna Bilous, Deepto Chakrabarty, Devarshi Choudhury, Alexander Dittmann, Sebastien Guillot, Alice Harding, Wynn Ho, Fred Lamb, Jim Lattimer, Renee Ludlam, Simin Mahmoodifar, Cole Miller, Sharon Morsink, Chanda Prescod-Weinstein, Paul Ray, Ron Remillard, Thomas Riley, Tuomo Salmi, Tod Strohmayer, Serena Vinciguerra, Anna Watts, Michael Wolff, Kent Wood.

Werner Israel and U of A students and postdocs, c 1991-93

From left to right: Alick Macpherson, Sharon Morsink, Alex Lyons, Werner Israel, Des McManus, Roberto Camporesi (?), Patrick Brady, Eric Poisson

Photographer and details unknown

Werner Israel's Interest in Neutron Stars

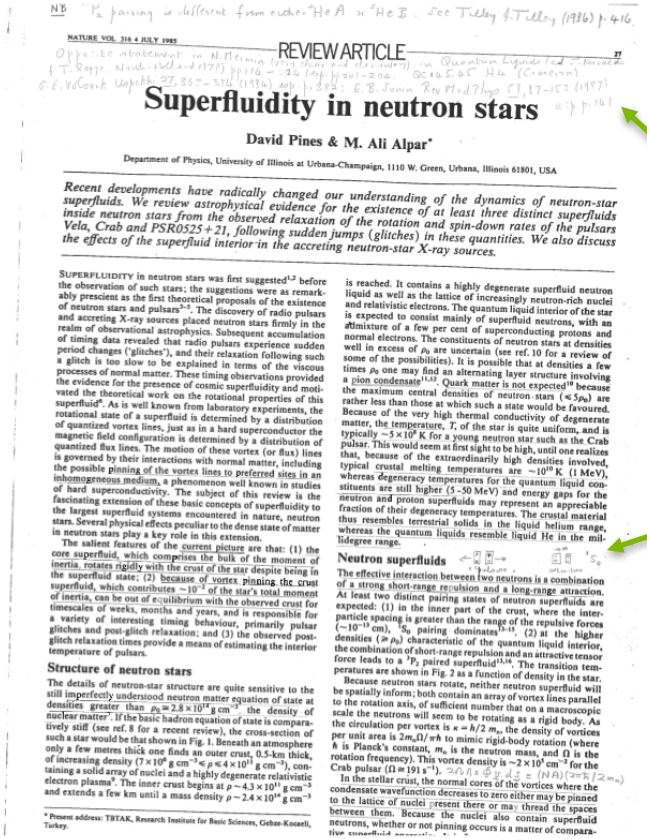

NATURE VOL. 316 4 JULY 1985 — REVIEW ARTICLE

Superfluidity in neutron stars

David Pines & M. Ali Alpar*
Department of Physics, University of Illinois at Urbana-Champaign, 1110 W. Green, Urbana, Illinois 61801, USA

Recent developments have radically changed our understanding of the dynamics of neutron-star superfluids. We review astrophysical evidence for the existence of at least three distinct superfluids inside neutron stars from the observed relaxation of the rotation and spin-down rates of the pulsars Vela, Crab and PSR0525+21, following sudden jumps (glitches) in these quantities. We also discuss the effects of the superfluid interior in the accreting neutron-star X-ray sources.

SUPERFLUIDITY in neutron stars was first suggested[1,2] before the observation of such stars; the suggestions were as remarkably prescient as the first theoretical proposals of the existence of neutron stars and pulsars[3–5]. The discovery of radio pulsars and accreting X-ray sources placed neutron stars firmly in the realm of observational astrophysics. Subsequent accumulation of timing data revealed that radio pulsars experience sudden period changes ('glitches'), and their relaxation following such a glitch is too slow to be explained in terms of the viscous processes of normal matter. These timing observations provided the evidence for the presence of cosmic superfluidity and motivated the theoretical work on the rotational properties of this superfluid[6]. As is well known from laboratory experiments, the rotational state of a superfluid is determined by a distribution of quantized vortex lines, just as in a hard superconductor the magnetic field configuration is determined by a distribution of quantized flux lines. The motion of these vortex (or flux) lines is governed by their interactions with normal matter, including the possible pinning of the vortex lines to preferred sites in an inhomogeneous medium, a phenomenon well known in studies of hard superconductivity. The subject of this review is the fascinating extension of these basic concepts of superfluidity to the largest superfluid systems encountered in nature, neutron stars. Several physical effects peculiar to the dense state of matter in neutron stars play a key role in this extension.

The salient features of the current picture are that: (1) the core superfluid, which comprises the bulk of the moment of inertia, rotates rigidly with the crust of the star despite being in the superfluid state; (2) because of vortex pinning the crust superfluid, which contributes $\sim 10^{-2}$ of the star's total moment of inertia, can be out of equilibrium with the observed crust for timescales of weeks, months and years, and is responsible for a variety of interesting timing behaviour, primarily pulsar glitches and post-glitch relaxation; and (3) the observed post-glitch relaxation times provide a means of estimating the interior temperature of pulsars.

Structure of neutron stars

The details of neutron-star structure are quite sensitive to the still imperfectly understood neutron matter equation of state at densities greater than $\rho_0 \approx 2.8 \times 10^{14}$ g cm^{-3}, the density of nuclear matter. If the basic hadron equation of state is comparatively stiff (see ref. 8 for a recent review), the cross-section of such a star would be that shown in Fig. 1. Beneath an atmosphere only a few metres thick one finds an outer crust, 0.5-km thick, of increasing density (7×10^6 g cm$^{-3} \leqslant \rho \leqslant 4 \times 10^{11}$ g cm^{-3}), containing a solid array of nuclei and a highly degenerate relativistic electron plasma[9]. The inner crust begins at $\rho \sim 4.3 \times 10^{11}$ g cm^{-3} and extends a few km until a mass density $\rho \sim 2.4 \times 10^{14}$ g cm^{-3} is reached. It contains a highly degenerate superfluid neutron liquid as well as the lattice of increasingly neutron-rich nuclei and relativistic electrons. The quantum liquid interior of the star is expected to consist mainly of superfluid neutrons, with an admixture of a few per cent of superconducting protons and normal electrons. The constituents of neutron stars at densities well in excess of ρ_0 are uncertain (see ref. 10 for a review of some of the possibilities). It is possible that at densities a few times ρ_0 one may find an alternating layer structure involving a pion condensate[11,12]. Quark matter is not expected[10] because the maximum central densities of neutron stars ($\leqslant 5\rho_0$) are rather less than those at which such a state would be favoured. Because of the very high thermal conductivity of degenerate matter, the temperature, T, of the star is quite uniform, and is typically $\sim 5 \times 10^8$ K for a young neutron star such as the Crab pulsar. This would seem at first sight to be high, until one realizes that, because of the extraordinarily high densities involved, typical crustal melting temperatures are $\sim 10^9$ K (1 MeV), whereas degeneracy temperatures for the quantum liquid constituents are still higher (5–50 MeV) and energy gaps for the neutron and proton superfluids may represent an appreciable fraction of their degeneracy temperatures. The crustal material thus resembles terrestrial solids in the liquid helium range, whereas the quantum liquids resemble liquid He in the milkidegree range.

Neutron superfluids

The effective interaction between two neutrons is a combination of a strong short-range repulsion and a long-range attraction. At least two distinct pairing states of neutron superfluids are expected: (1) in the inner part of the crust, where the interparticle spacing is greater than the range of the repulsive forces ($\sim 10^{-13}$ cm), $^1S_0$ pairing dominates[13–15]. (2) at the higher densities ($\geqslant \rho_0$) characteristic of the quantum liquid interior, the combination of short-range repulsion and an attractive tensor force leads to a $^3P_2$ paired superfluid[13,16]. The transition temperatures are shown in Fig. 2 as a function of density in the star.

Because neutron stars rotate, neither neutron superfluid will be spatially inform; both contain an array of vortex lines parallel to the rotation axis, of sufficient number that on a macroscopic scale the neutrons will seem to be rotating as a rigid body. As the circulation per vortex is $\kappa = h/2m_n$, the density of vortices per unit area is $2m_n\Omega/\pi\hbar$ to mimic rigid-body rotation (where $\hbar$ is Planck's constant, m_n is the neutron mass, and Ω is the rotation frequency). This vortex density is $\sim 2 \times 10^5$ cm^{-2} for the Crab pulsar ($\Omega = 191$ s^{-1}).

In the stellar crust, the normal cores of the vortices where the condensate wavefunction decreases to zero either may be pinned to the lattice of nuclei present there or may thread the spaces between them. Because the nuclei also contain superfluid neutrons, whether or not pinning occurs is a matter of compara-

* Present address: TBTAK, Research Institute for Basic Sciences, Gebze-Kocaeli, Turkey.

Werner's annotations on a paper that he found interesting!

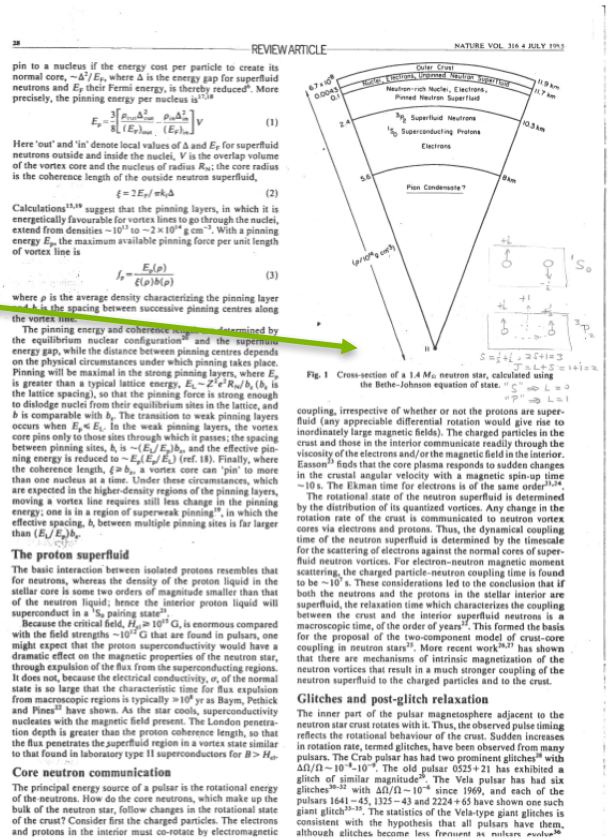

REVIEW ARTICLE — NATURE VOL. 316 4 JULY 1985

pin to a nucleus if the energy cost per particle to create its normal core, $\sim\Delta^2/E_F$, where Δ is the energy gap for superfluid neutrons and E_F their Fermi energy, is thereby reduced[6]. More precisely, the pinning energy per nucleus is[17,18]

$$E_p = \frac{3}{8}\left[\frac{\rho_{\rm out}\Delta^2_{\rm out}}{(E_F)_{\rm out}} - \frac{\rho_{\rm in}\Delta^2_{\rm in}}{(E_F)_{\rm in}}\right]V \qquad (1)$$

Here 'out' and 'in' denote local values of Δ and E_F for superfluid neutrons outside and inside the nuclei, V is the overlap volume of the vortex core and the nucleus of radius R_N; the core radius is the coherence length of the outside neutron superfluid,

$$\xi = 2E_{Fj}/\pi k_j\Delta \qquad (2)$$

Calculations[15,19] suggest that the pinning layers, in which it is energetically favourable for vortex lines to go through the nuclei, extend from densities $\sim 10^{13}$ to $\sim 2 \times 10^{14}$ g cm^{-3}. With a pinning energy E_p, the maximum available pinning force per unit length of vortex line is

$$f_p = \frac{E_p(\rho)}{\xi(\rho)b(\rho)} \qquad (3)$$

where ρ is the average density characterizing the pinning layer and b is the spacing between successive pinning centres along the vortex line.

The pinning energy and coherence length, determined by the equilibrium nuclear configuration[20] and the superfluid energy gap, while the distance between pinning centres depends on the physical circumstances under which pinning takes place. Pinning will be maximal in the strong pinning layers, where E_p is greater than a typical lattice energy, $E_L \sim Z^2e^2R_{\rm wc}/b_\perp$ ($b_\perp$ is the lattice spacing), so that the pinning force is strong enough to dislodge nuclei from their equilibrium sites in the lattice, and b is comparable with $b_\perp$. The transition to weak pinning layers occurs when $E_p \ll E_L$. In the weak pinning layers, the vortex core pins only to those sites through which it passes; the spacing between pinning sites, $b_\parallel \approx (E_L/E_p)b_\perp$, and the effective pinning energy is reduced to $\sim E_p(E_p/E_L)$ (ref. 18). Finally, where the coherence length, $\xi \gg b_\perp$, a vortex core can 'pin' to more than one nucleus at a time. Under these circumstances, which are expected in the higher-density regions of the pinning layers, moving a vortex line requires still less change in the pinning energy; one is in a region of superweak pinning[18], in which the effective spacing, b, between multiple pinning sites is far larger than $(E_L/E_p)b_\perp$.

The proton superfluid

The basic interaction between isolated protons resembles that for neutrons, whereas the density of the proton liquid in the stellar core is some two orders of magnitude smaller than that of the neutron liquid; hence the interior proton liquid will superconduct in a $^1S_0$ pairing state[21].

Because the critical field, $H_{c2} \geqslant 10^{15}$ G, is enormous compared with the field strengths $\sim 10^{12}$ G that are found in pulsars, one might expect that the proton superconductivity would have a dramatic effect on the magnetic properties of the neutron star, through expulsion of the flux from the superconducting regions. It does not, because the electrical conductivity, σ, of the normal state is so large that the characteristic time for flux expulsion from macroscopic regions is typically $\gg 10^8$ yr as Baym, Pethick and Pines[22] have shown. As the star cools, superconductivity nucleates with the magnetic field present. The London penetration depth is greater than the proton coherence length, so that the flux penetrates the superfluid region in a vortex state similar to that found in laboratory type II superconductors for $B > H_{c1}$.

Core neutron communication

The principal energy source of a pulsar is the rotational energy of the neutrons. How do the core neutrons, which make up the bulk of the neutron star, follow changes in the rotational state of the crust? Consider first the charged particles. The electrons and protons in the interior must co-rotate by electromagnetic coupling, irrespective of whether or not the protons are superfluid (any appreciable differential rotation would give rise to inordinately large magnetic fields). The charged particles in the crust and those in the interior communicate readily through the viscosity of the electrons and/or the magnetic field in the interior. Easson[23] finds that the core plasma responds to sudden changes in the crustal angular velocity with a magnetic spin-up time ~ 10 s. The Ekman time for electrons is of the same order[23,24].

The rotational state of the neutron superfluid is determined by the distribution of its quantized vortices. Any change in the rotation rate of the crust is communicated to neutron vortex cores via electrons and protons. Thus, the dynamical coupling time of the neutron superfluid is determined by the timescale for the scattering of electrons against the normal cores of superfluid neutron vortices. For electron–neutron magnetic moment scattering, the charged particle–neutron coupling time is found to be $\sim 10^3$ s. These considerations led to the conclusion that if both the neutrons and the protons in the stellar interior are superfluid, the relaxation time which characterizes the coupling between the crust and the interior superfluid neutrons is a macroscopic time, of the order of years[22]. This formed the basis for the proposal of the two-component model of crust-core coupling in neutron stars[25]. More recent work[26,27] has shown that there are mechanisms of intrinsic magnetization of the neutron vortices that result in a much stronger coupling of the neutron superfluid to the charged particles and to the crust.

Glitches and post-glitch relaxation

The inner part of the pulsar magnetosphere adjacent to the neutron star crust rotates with it. Thus, the observed pulse timing reflects the rotational behaviour of the crust. Sudden increases in rotation rate, termed glitches, have been observed from many pulsars. The Crab pulsar has had two prominent glitches[28] with $\Delta\Omega/\Omega \sim 10^{-8}$–$10^{-6}$. The old pulsar 0525+21 has exhibited a glitch of similar magnitude[29]. The Vela pulsar has had six glitches[30–32] with $\Delta\Omega/\Omega \sim 10^{-6}$ since 1969, and each of the pulsars 1641−45, 1325−43 and 2224+65 have shown one such giant glitch[33–35]. The statistics of the Vela-type giant glitches is consistent with the hypothesis that all pulsars have them, although glitches become less frequent as pulsars evolve[36]

Fig. 1 Cross-section of a 1.4 $M_\odot$ neutron star, calculated using the Bethe–Johnson equation of state.

Do vortex filaments in a superfluid neutron star produce gravimagnetic forces? Balasin & Israel, CQG 1999

Covariant fluid dynamics, nonequilibrium thermodynamics, kinetic theory, superfluidity – many papers!

The neutron star interior

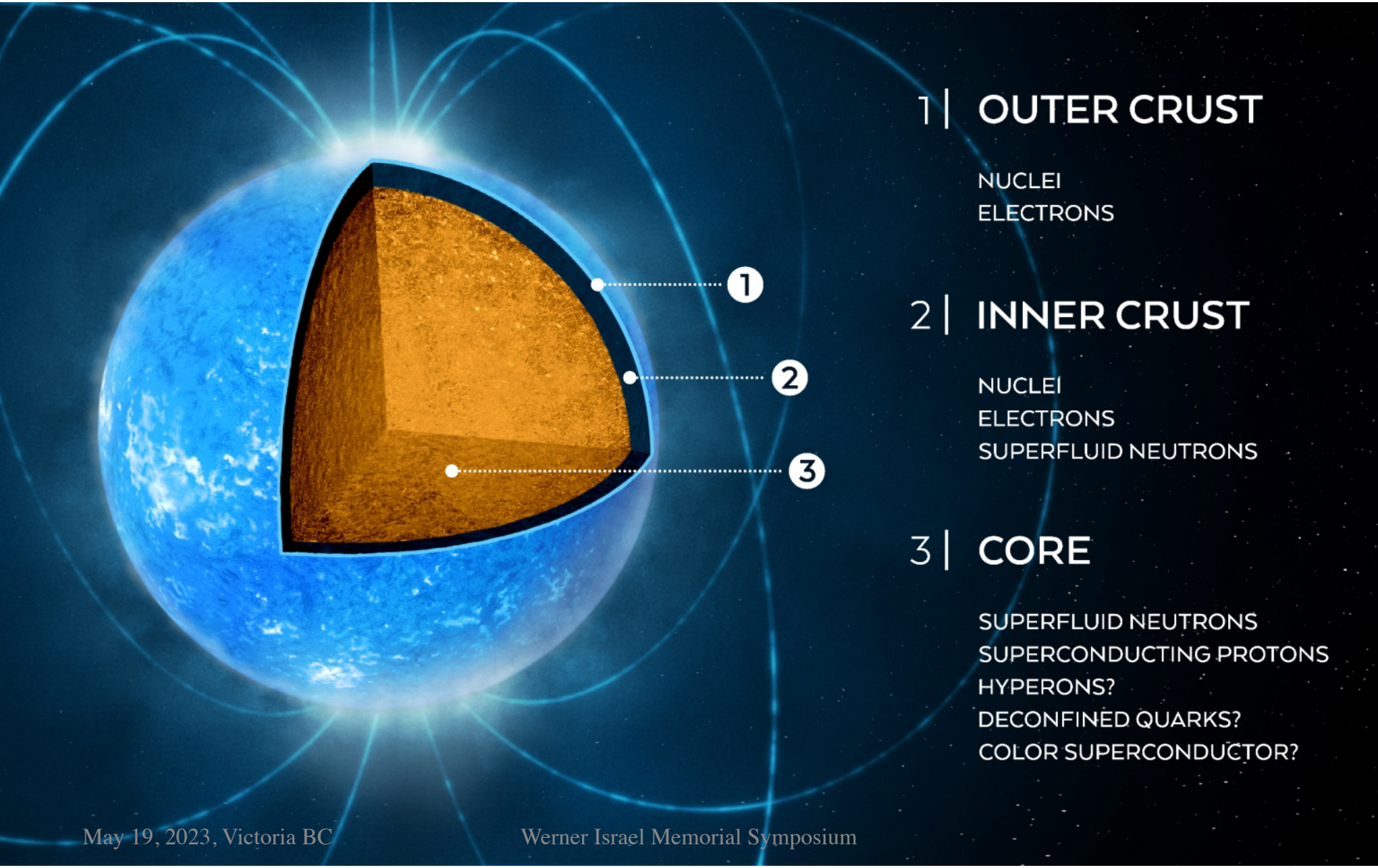

Possible Phase Diagram for Dense Matter

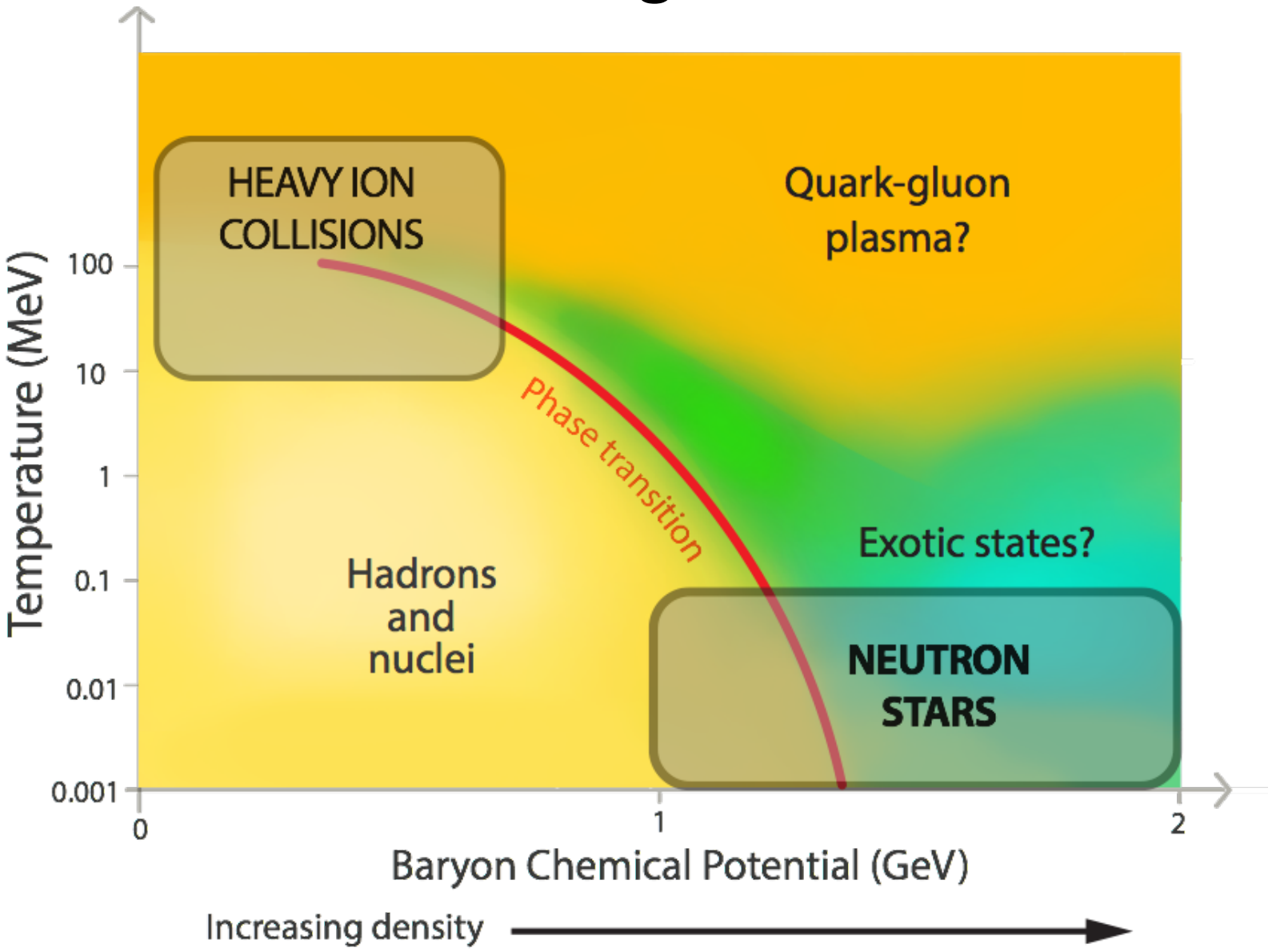

Equations of State vs Mass-Radius Curves

Stellar structure equations

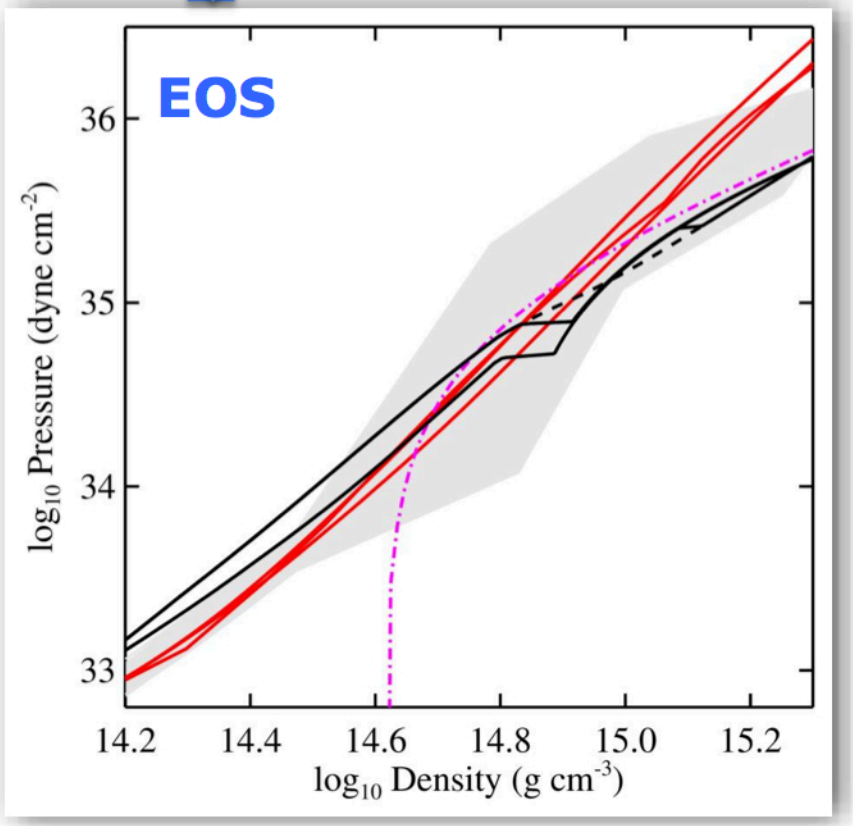

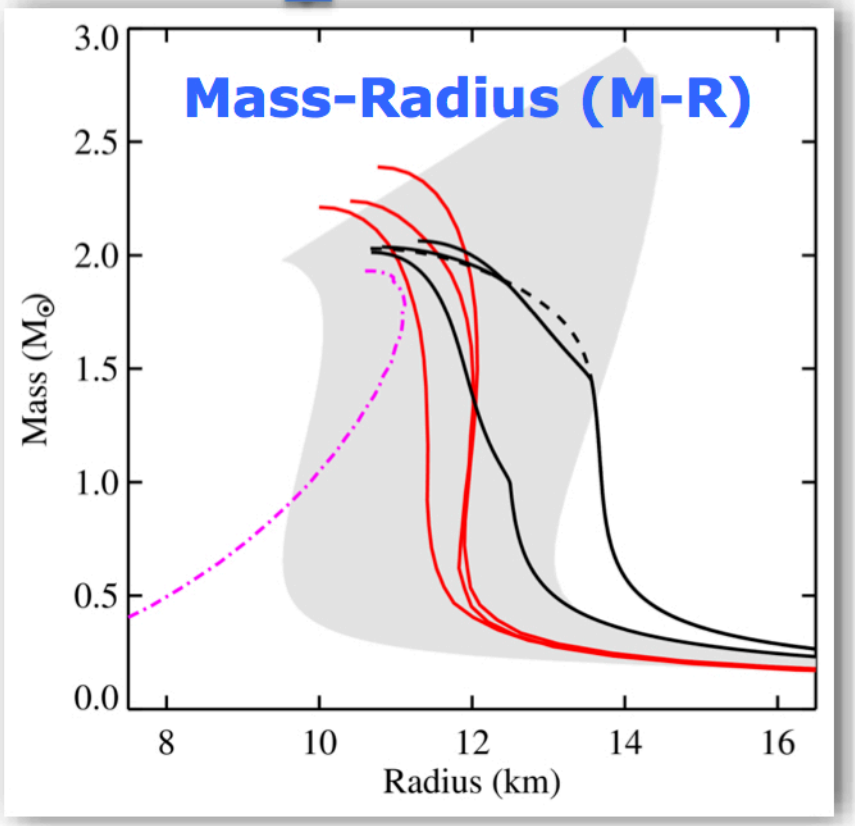

What do we measure???

- We talk about “measuring” mass and radius to constrain the EOS
- But what do we mean by a measurement?
- We don’t really measure mass or radius – Instead we measure other quantities and use a physical model that depends on M and/or R
- Models range from simple (just gravity) to complicated (atmosphere models; stellar astrophysics; transport properties; dynamical gravity; etc…)

Types of Neutron Star Observations (Past, Present, Future)

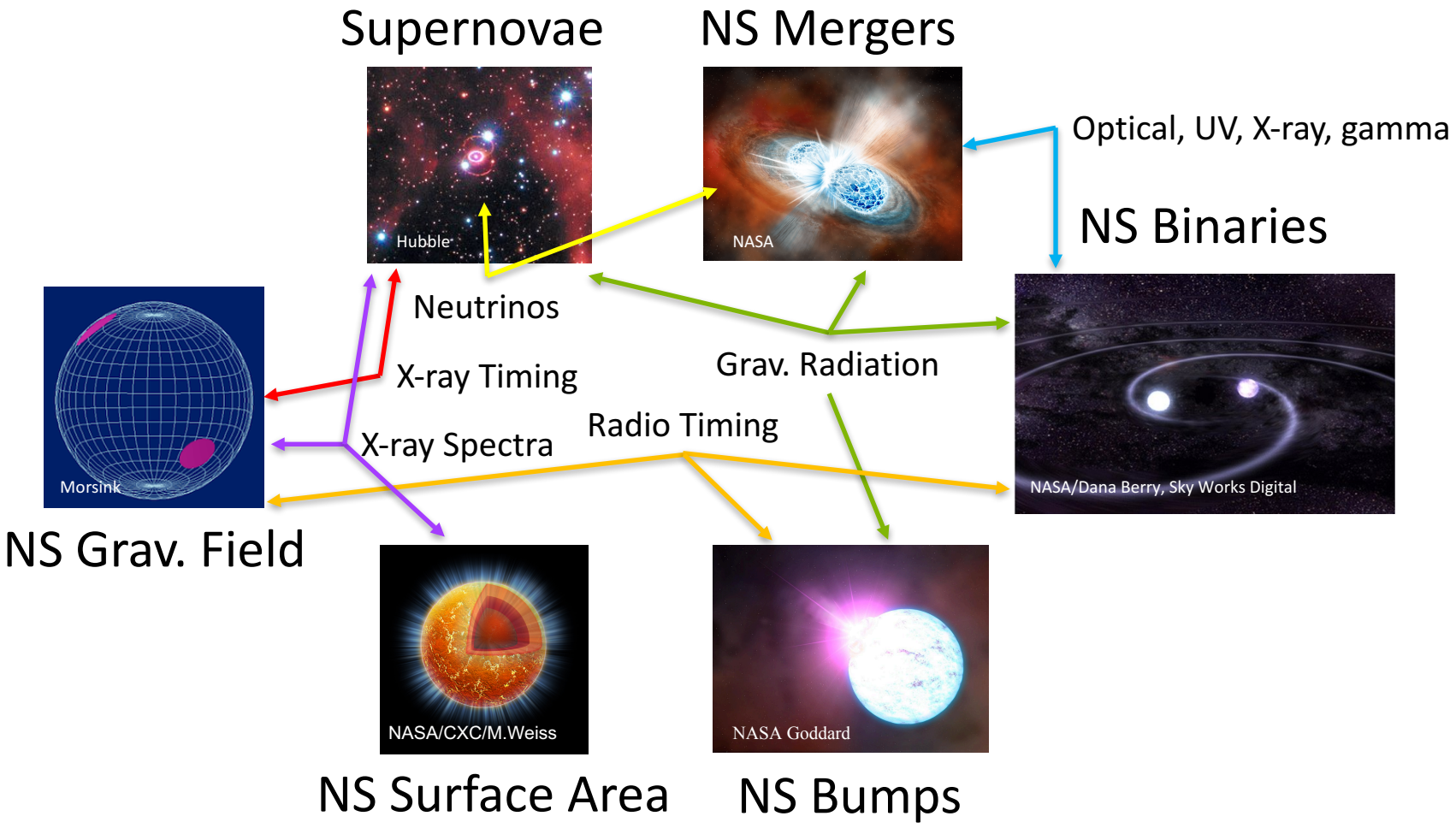

MASS MEASUREMENTS

The neutron star mass-radius relation

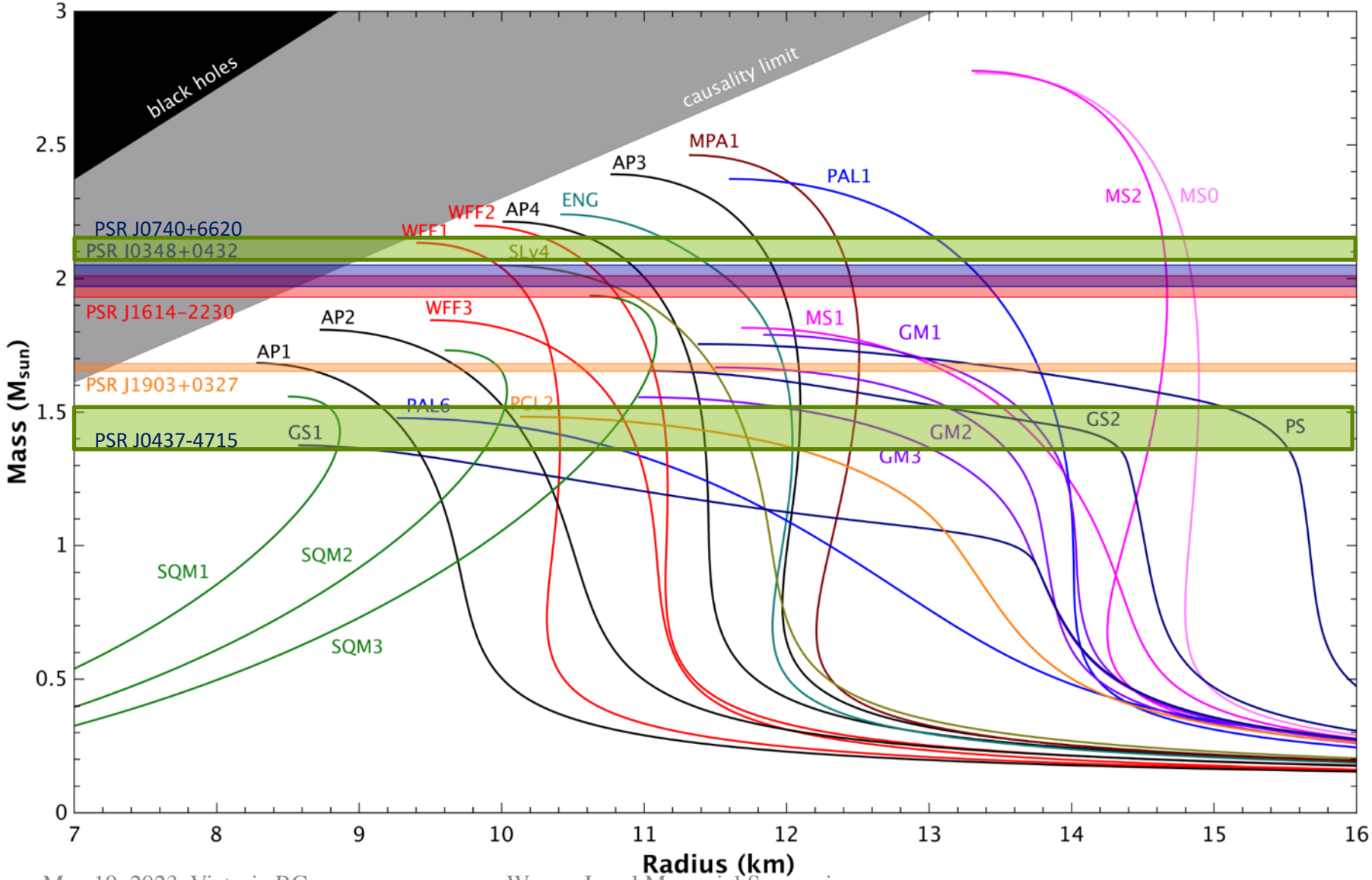

Credit: N. Wex

RADIUS MEASUREMENTS

Hubble's Best NS Photo

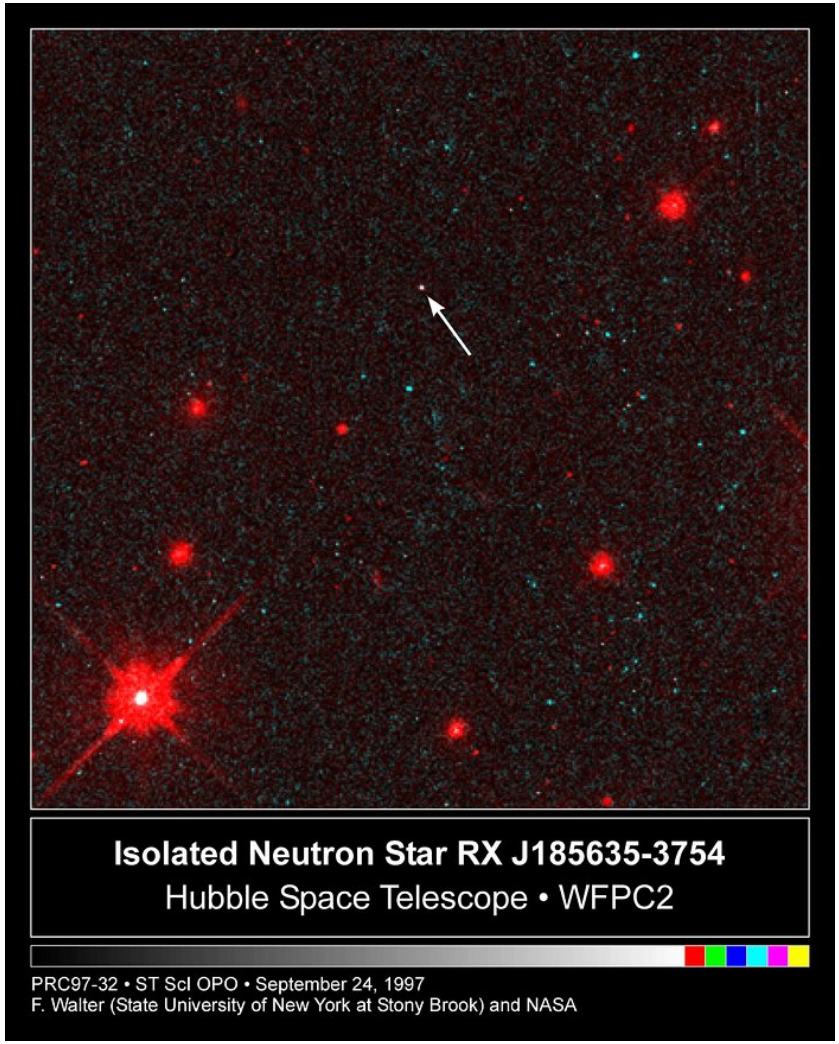

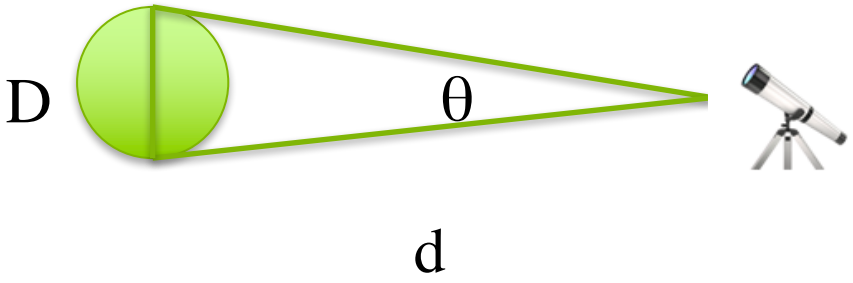

Direct geometrical measurement:
$D = \theta d$ not possible!

FINITE SIZE EFFECTS IN BINARIES

NS Finite Size Effects in NS-NS Inspiral (GW measurements)

- NS is not a point particle!
- Orbital energy during binary inspiral is ``wasted" in tidal deformations or exciting oscillation modes
- Compare GW phase evolution with point particle predictions to find the NS finite size
- Leads to limits on Tidal Deformability, Λ

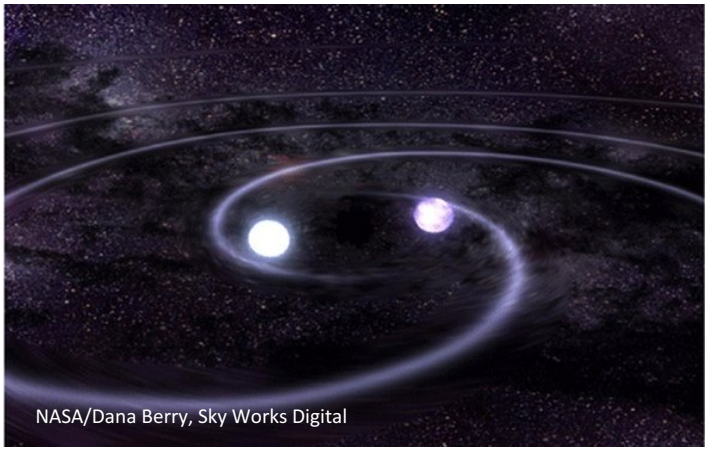

Love Number related to NS Radius

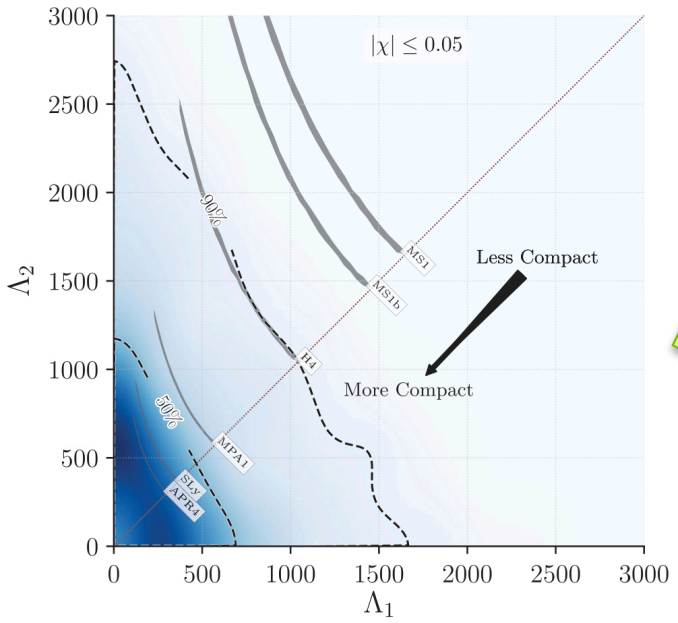

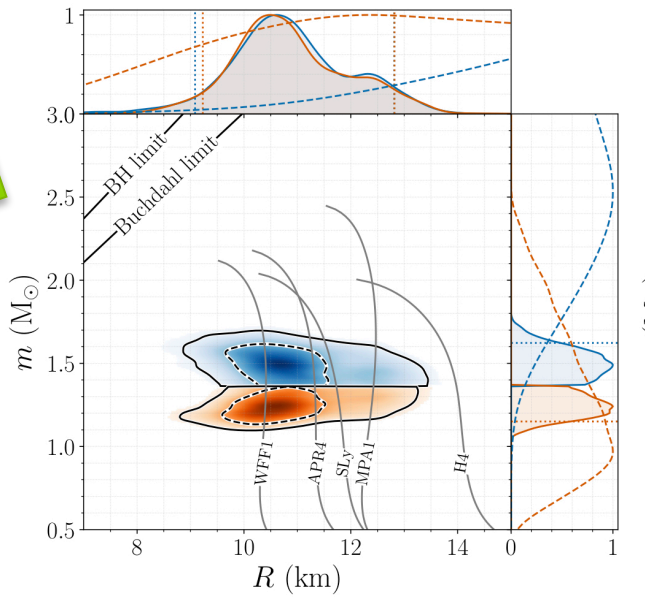

LIGO observations "prefer" smaller NS radii!

Abbott+ PRL 2017, 2018

PULSE PROFILE MODELLING

Pulse Profile Modelling

- Hot spots on rotating neutron star
- X-rays feel the NSs gravitational field while travelling from star to telescope
- Gravitational Potential ~ M/R causes light to travel on curved path
- Doppler Boosting ~ Ω R/c adds timing asymmetry and harmonics

Rotation-Powered Millisecond Period Pulsars

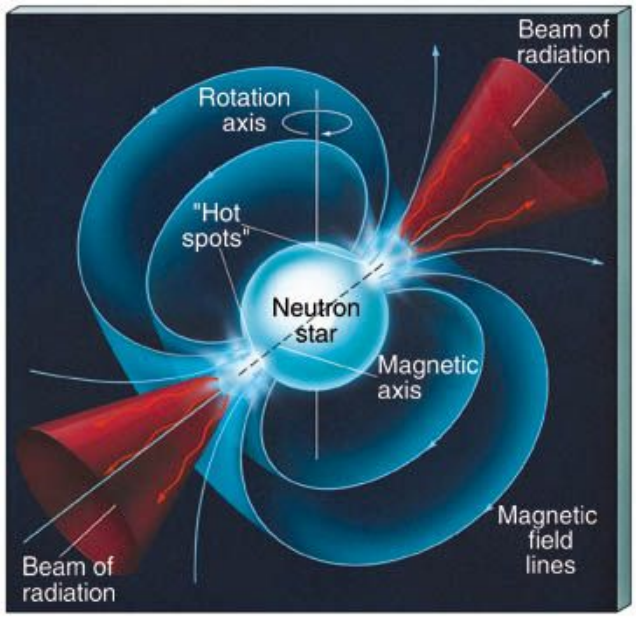

- Radio and X-ray pulsations
- Radio beam (far from star) produces electron-positron ``return currents" that heat the star's surface creating hot spots

- $\dot{E} \approx 10^{33–34}$ erg/s, $L_X \approx 10^{30–31}$ erg/s
- Soft, thermal X-ray emission from hot spots
- Non-magnetic (0 G, effectively $B < 10^{10}$ G) hydrogen or helium atmosphere
- **Non-transient (always "on") and non-variable**

Model Geometry and Relativistic Effects

- Rotating star with oblate shape
- Two or more X-ray emitting "hot-spots"
- Relativistic effects:
  - Light bending in a Schwarzschild geometry
  - Gravitational redshift
  - Doppler shifts
  - Relativistic aberration
  - Propagation time differences

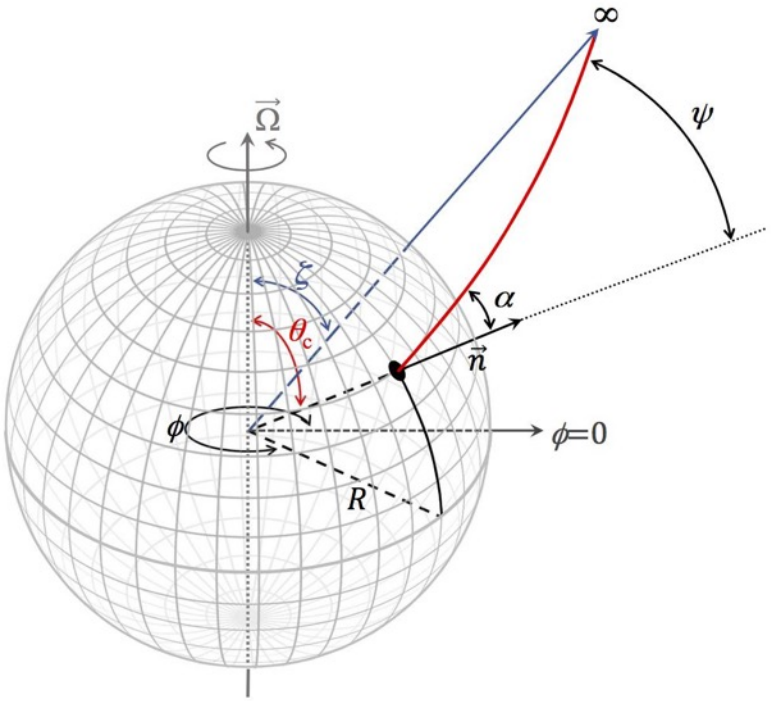

- Spot co-latitudes θ_{c1} , θ_{c2}, …
- Relative phase of the spots
- Spot angular radii $\rho_{1,2}$
- Observer inclination ζ
- Relation between ψ and α depends on M/R

(Miller & Lamb 1998; Beloborodov 2002; Poutanen & Gierlinski 2003; Poutanen & Beloborodov 2006; Morsink et al. 2007; Lo et al. 2013; Miller & Lamb 2015; Bogdanov; Ozel & Psaltis et al. ; Strohmayer & Mahmoodifar; Watts et al. , …)

Dependence of Pulse Profiles on M/R

M/R = “compactness” affects light-bending

Larger M/R → less modulation

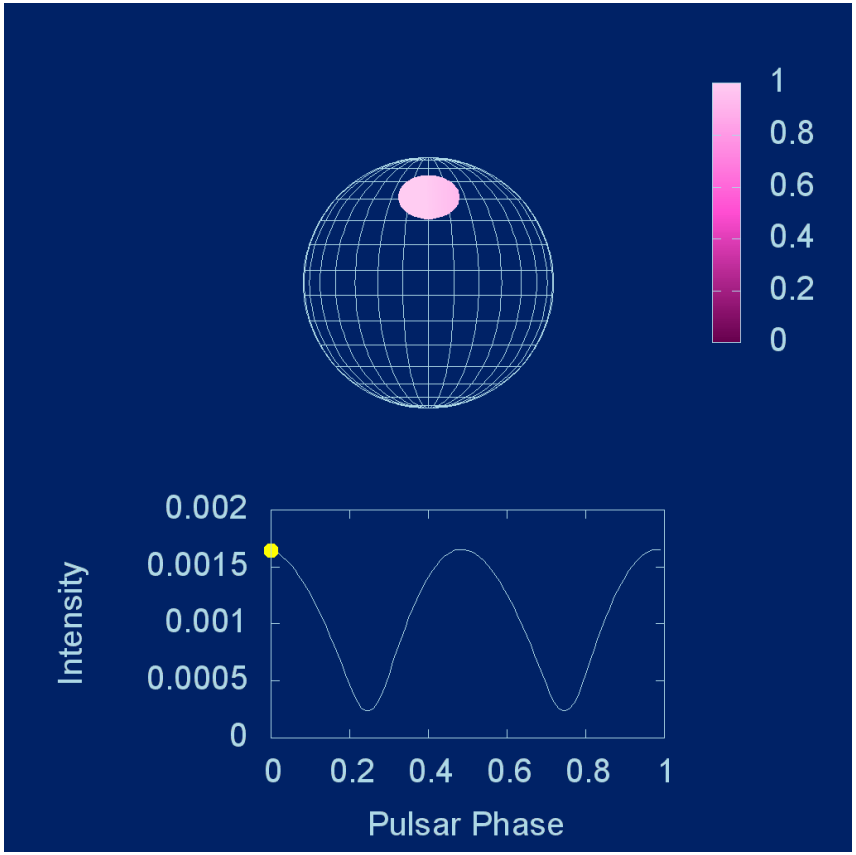

Newtonian Gravity

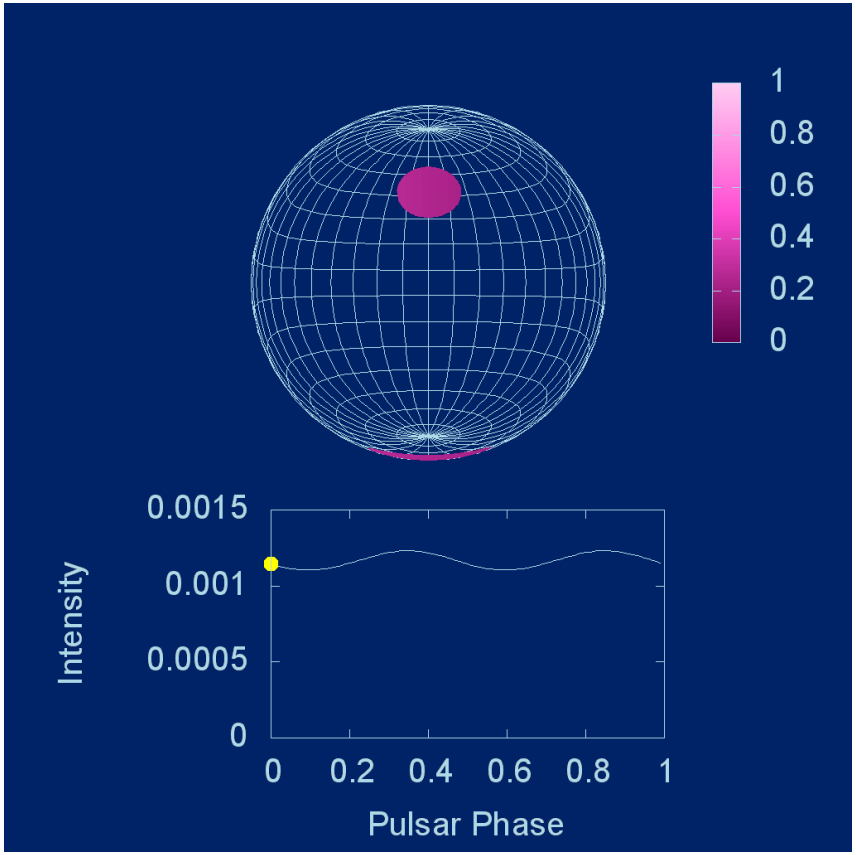

General Relativity M/R = 0.25

Effect of Observer's Viewing Angle

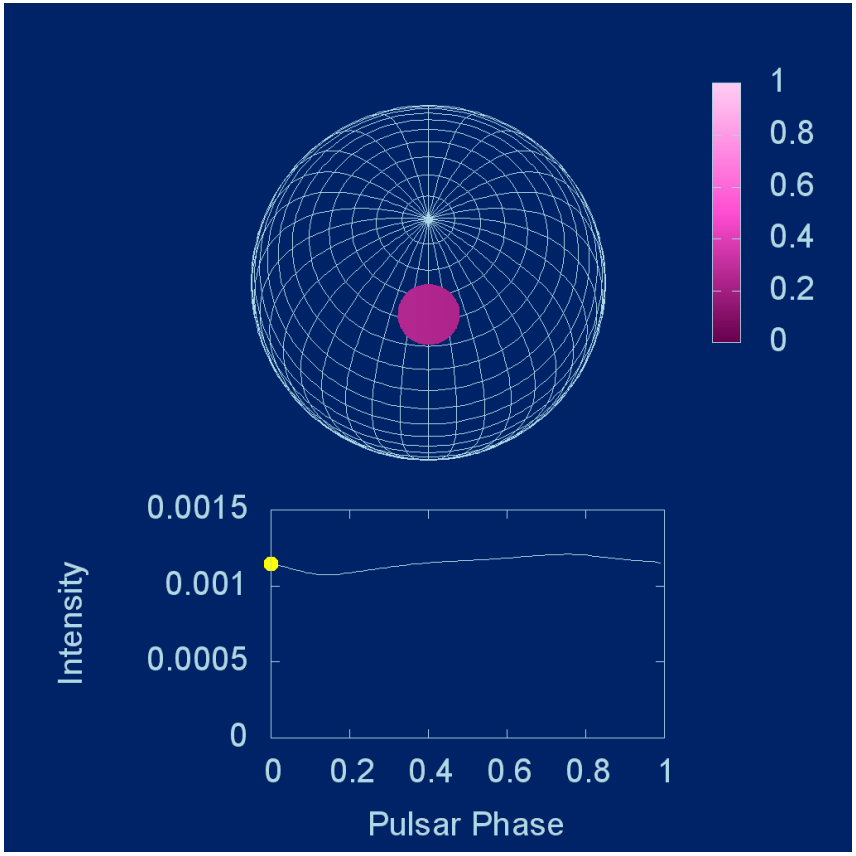

30 deg from Spin Axis

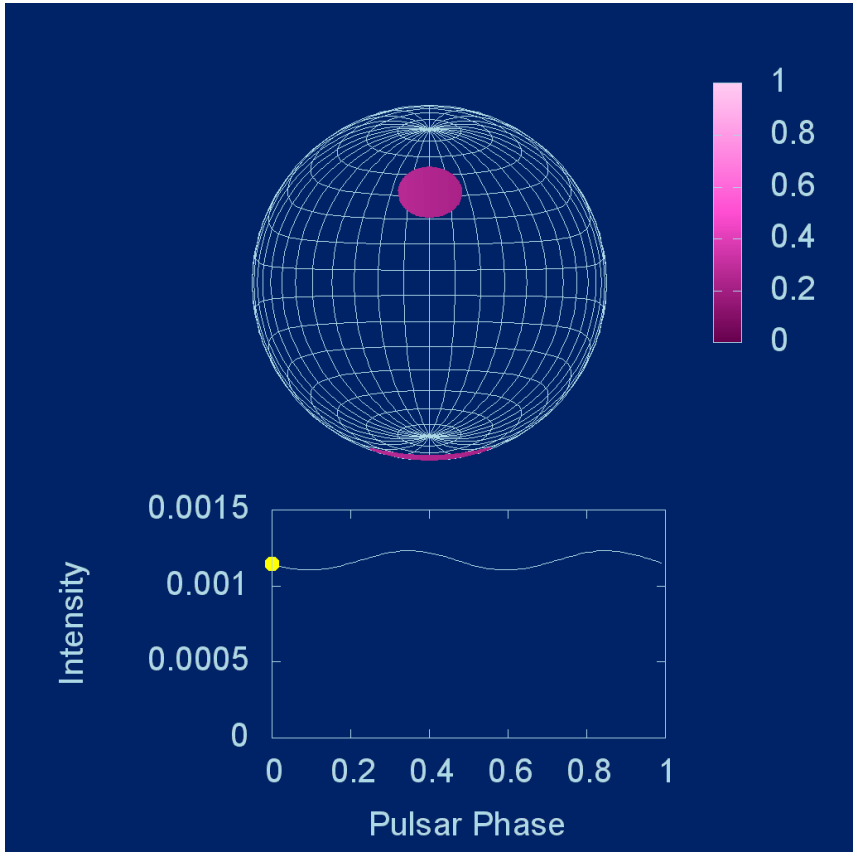

90 deg from Spin Axis

Effect of Rotational Speed $\propto$ R sini sinθ

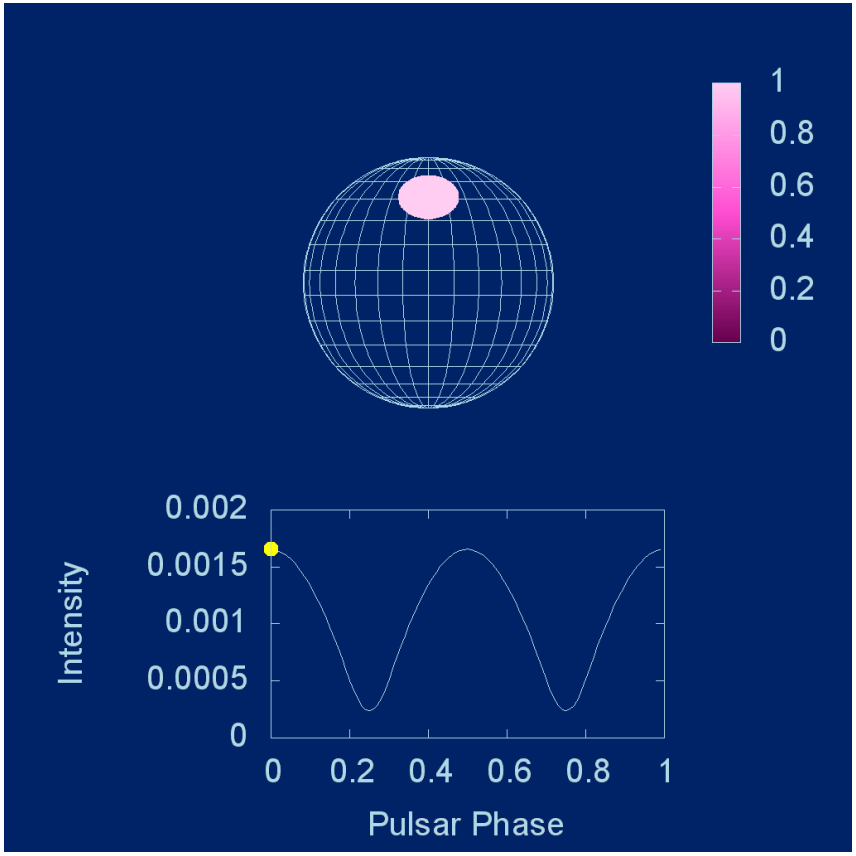

v/c = 0.01

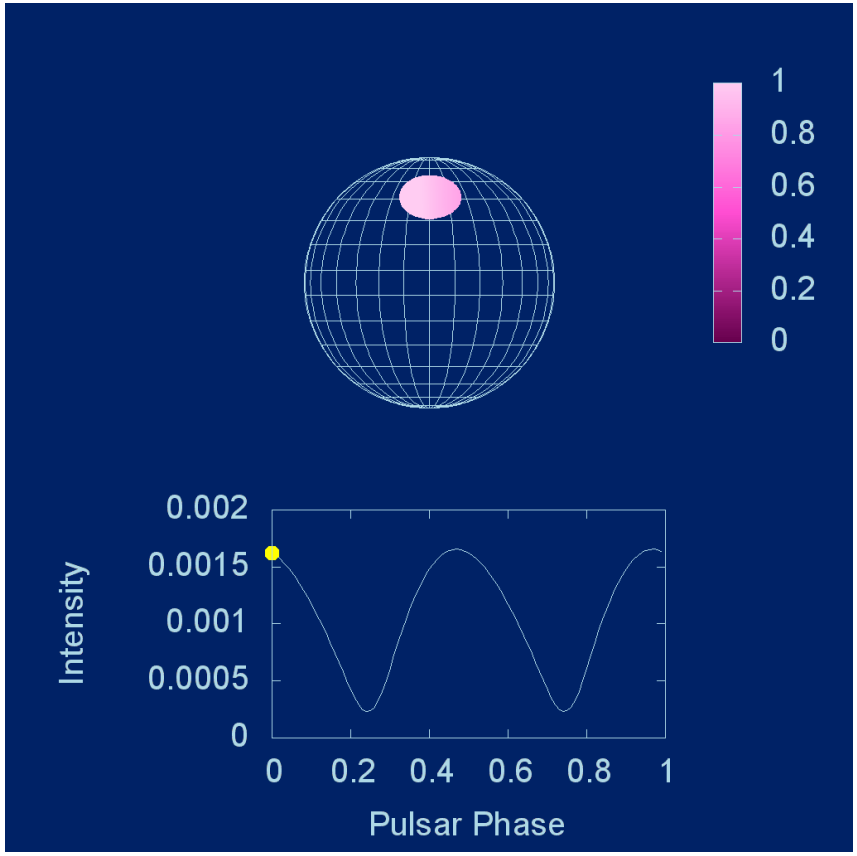

v/c = 0.2 (harmonics)

Metric for axisymmetric and stationary star

$$ds^2 = -e^{\gamma+\rho}dt^2 + e^{2\alpha}\left(dr^2 + r^2 d\theta^2\right) + e^{\gamma-\rho}r^2\sin^2\theta(d\phi - \omega dt)^2$$

- Metric functions γ, ρ, α, ω are functions of r and θ
- Metric computed numerically on 2D grid using Green function method (rns code by Nikolaos Stergioulas, based on code by Greg Cook and method by Komatsu, Eriguchi and Hachisu, 1989)
- Raytracing on numerical background to construct pulse shapes to compare with approximations based on Schwarzschild and Kerr metrics. (Cadeau, Morsink, Leahy, & Campbell ApJ 2007)
- Test of Schwarzschild + Doppler Approximation

Spot at 15° from North Pole Observer at 100° from North Pole

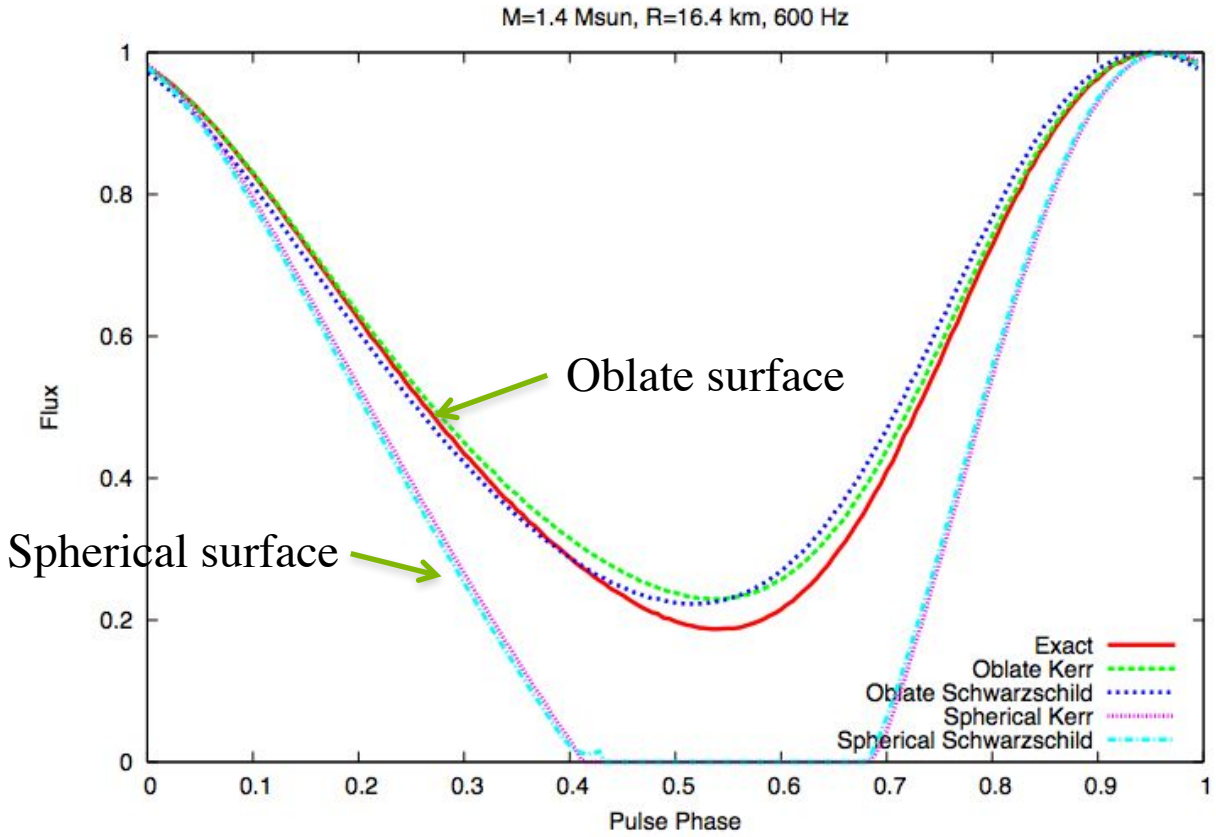

(Cadeau, Morsink, Leahy, & Campbell ApJ 2007)

How Oblate is a Neutron Star?

Fraction of Breakup Frequency: $\frac{2\pi}{P}\sqrt{\frac{R^3}{GM}}$

Neutron Stars with M=1.4 M_{sun}, R=12 km

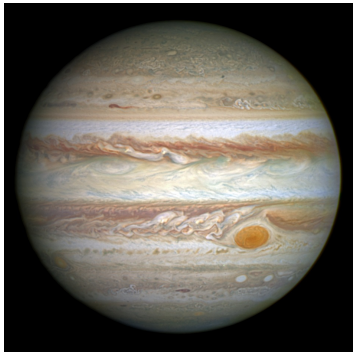

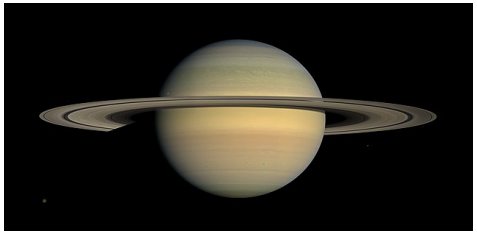

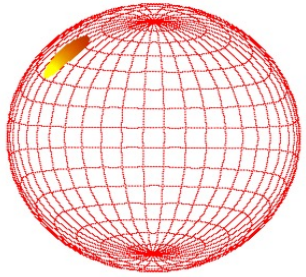

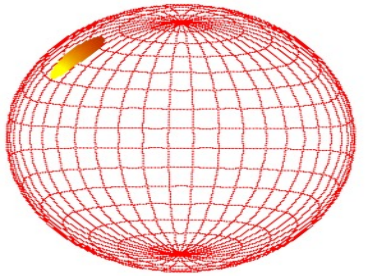

Planet images: NASA

P = 9.9 hrs

$\frac{2\pi}{P}\sqrt{\frac{R^3}{GM}} = 0.3$

P = 10.5 hrs

$\frac{2\pi}{P}\sqrt{\frac{R^3}{GM}} = 0.4$

P = 3 ms

$\frac{2\pi}{P}\sqrt{\frac{R^3}{GM}} = 0.2$

v/c = 0.085

P = 1.5 ms

$\frac{2\pi}{P}\sqrt{\frac{R^3}{GM}} = 0.4$

v/c = 0.17

Stellar Oblateness

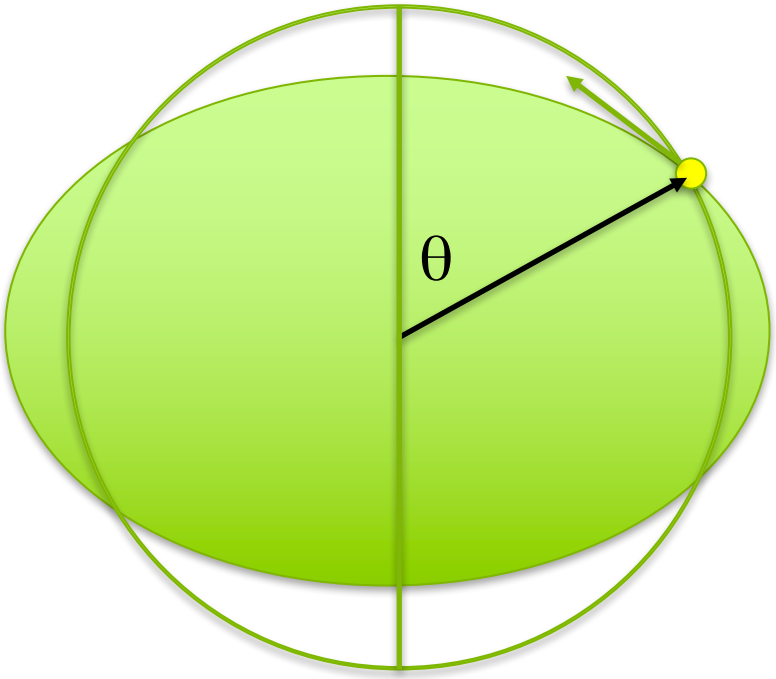

Morsink, Leahy, Cadeau & Braga 2007 ApJ

Digression on Black Hole "No Hair"

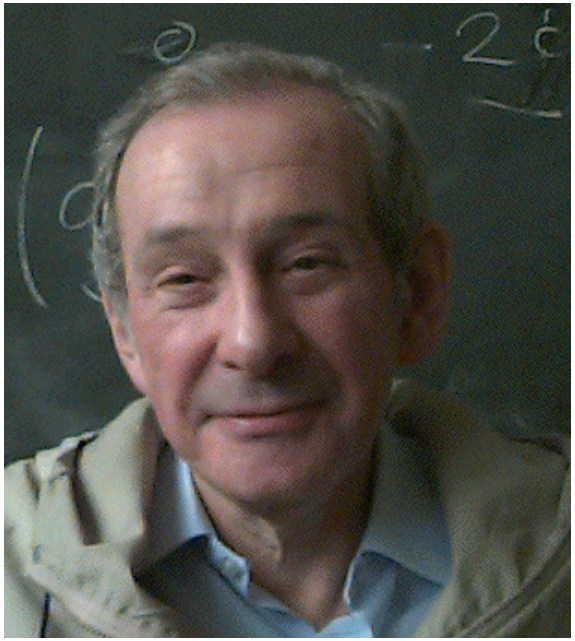

Werner Israel

- Black holes are very simple!
- Describe a rotating BH with 2 parameters: M, a
- Event Horizon radius given by:

  $R_{EH} = 2M + M[(1-(a/M)^2)^{1/2} -1]$
- Gravitational field outside of BH:

  $\Phi(r,\theta) = - M/r + \Phi_2/r^3 P_2(\cos\theta) + \ldots$

  $\Phi_2 = M a^2$
- Properties of a BH are independent of the properties of the stuff that formed it.

Neutron Stars Have “Hair”

- Given a mass and spin (M and Ω) different EOS predict different Radii (R)
- However, given M, R, Ω dimensionless quantities: $x = GM/Rc^2$ $y = \Omega^2 R^3/GM$
- Many secondary NS properties depend only on x, y.
- Eg: Moment of Inertia (Ravenhall & Pethick, 1994)
- I Love Q (Moment of Inertia, Love number, Quadrupole moment) relationships (Yagi & Yunes 2013)
- “Neutron Star Universality”

Stellar Oblateness

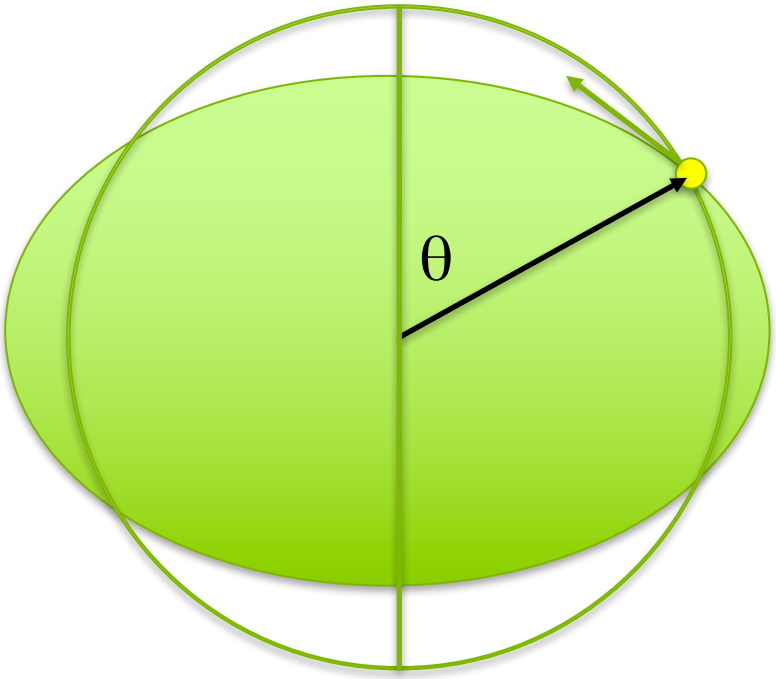

"Universal" form for oblate shape:
$R(\theta) = R_e - b \cos^2\theta$

$b = b(M/R_e, \Omega^2 R_e^3/GM)$

No new parameters required!

Motivation for the Oblate Schwarzschild Approximation

Morsink, Leahy, Cadeau & Braga 2007 ApJ

X-ray Timing Telescopes

- RXTE – Rossi X-ray Timing Explorer (1995-2012) X-ray timing
- XMM – great energy resolution, +timing mode
- AstroSAT – Indian RXTE-like mission
- **NICER – great timing AND spectroscopy – designed for pulse profile observations!!!!**
- Future:
  - eXTP, StrobeX = RXTE x 10 + spectra
    + polarization (eXTP)!!!

The Neutron Star Interior Composition Explorer

PI: Keith Gendreau

Science Lead: Zaven Arzoumanian

Installed on the ISS in June 2017

NICER Target List for M-R Constraints

	Spin Period (ms)	Distance (pc)	Mass * ($M_\odot$)	NICER Rate (photons/ks)
PSR J0437−4715	5.76	156.79±0.25	1.44±0.07	1319
PSR J0030+0451	4.87	325±9	isolated	314
PSR J1231−1411	3.68	440	?	210
PSR J2124−3358	4.93	410_{-70}^{+90}	isolated	100
PSR J0614−3329	3.10	~ 550	?	27
PSR J1614−2230	3.15	670_{-40}^{+50}	1.928±0.016	18
PSR J0740+6620	2.89	1140_{-150}^{+170}	2.08±0.07	15

* Masses from radio timing for pulsars in a binary.

NICER Target List for M-R Constraints

	Spin Period (ms)	Distance (pc)	Mass * ($M_\odot$)	NICER Rate (photons/ks)
PSR J0437−4715	5.76	156.79±0.25	1.44±0.07	1319
Expect results later in 2023! Best statistics on this one!				
PSR J0030+0451	4.87	325±9	isolated	314
ApJL 2019, inferred mass near 1.4 M_{sun}, 1.9 Msec exposure in 2019				
PSR J1231−1411	3.68	440	?	210
Fermi LAT gamma ray pulsar, X-ray pulsations 1st detected by NICER!				
PSR J2124−3358	4.93	410_{-70}^{+90}	isolated	100
PSR J0614−3329	3.10	~ 550	?	27
PSR J1614−2230	3.15	670_{-40}^{+50}	1.928±0.016	18
PSR J0740+6620	2.89	1140_{-150}^{+170}	2.08±0.07	15
ApJL 2021, high mass, denser interior important for supra-nuclear physics!				

* Masses from radio timing for pulsars in a binary.

J0030 Lightcurve (2019 dataset)

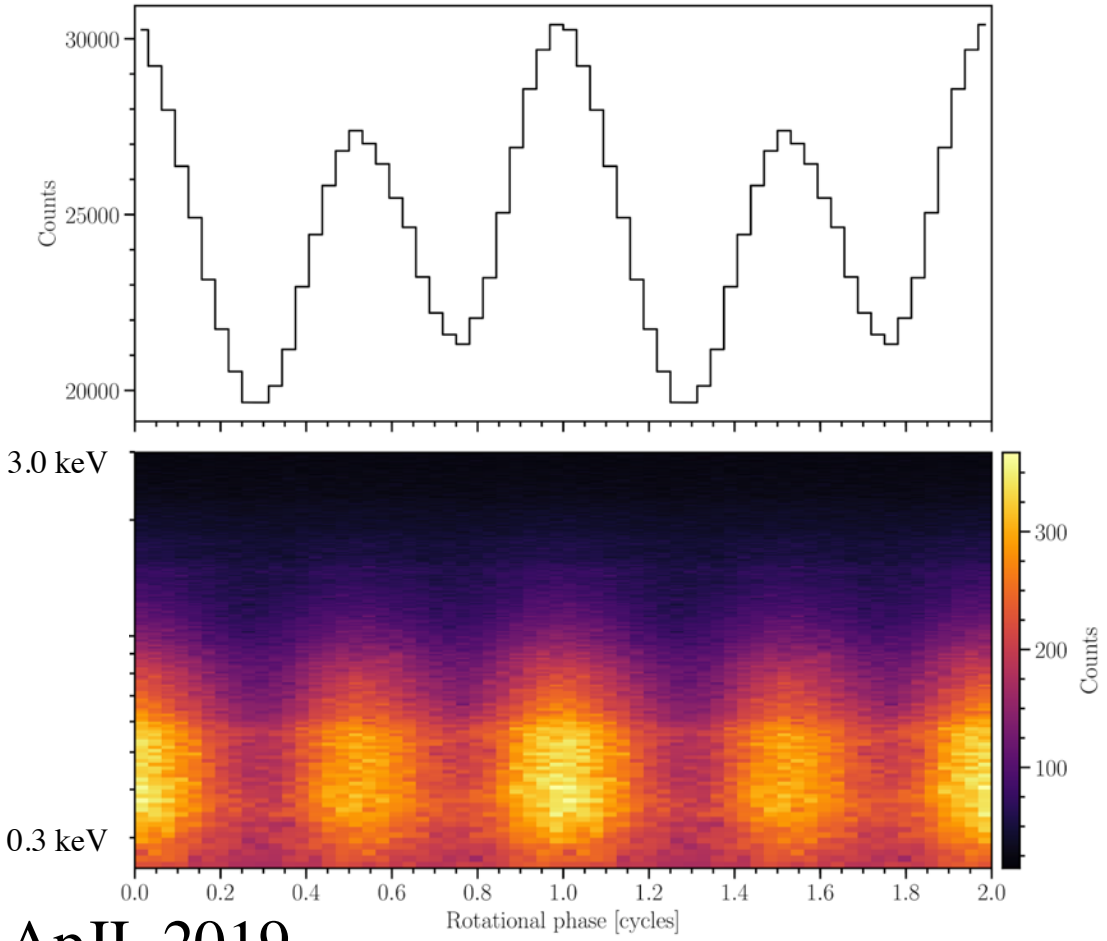

Bogdanov+, ApJL 2019

First Results on J0030

- No independent radio mass measurement
- Two independent analyses (crescents or ovals) Riley+ (ApJL 2019) and Miller+ (ApJL 2019)

M = $1.34^{+0.15}_{-0.16}$ M_{sun} R = $12.71^{+1.14}_{-1.19}$ km (Riley+)
M = $1.44^{+0.15}_{-0.14}$ M_{sun} R = $13.02^{+1.24}_{-1.06}$ km (Miller+)

- Similar observer inclinations, and spot locations
- Differences in M, R values show systematics in modelling choices
- Updated values (more observing time, improved background) expected later in 2023
- Error regions will shrink with better statistics!

Inferred Spot Geometries

observer

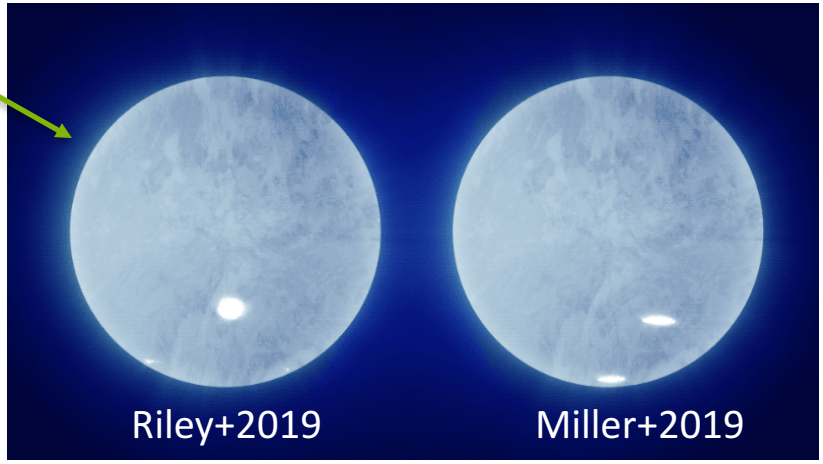

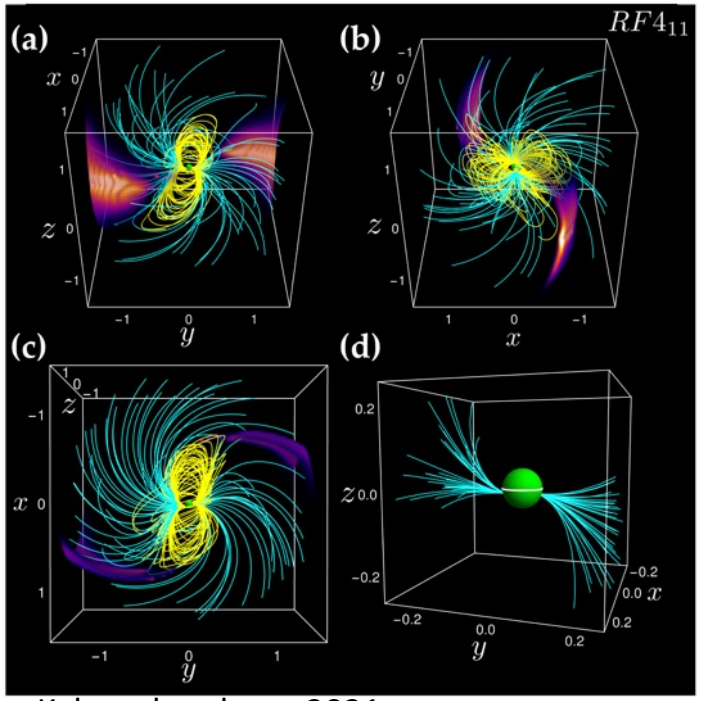

Kalapotharakos + 2021

- Non-dipole magnetic field
- Example: Offset dipole + quadrupole
- Kalapotharakos, Wadiasingh, Harding, & Kazanas ApJ (2021)

PSR J0740 Lightcurve

Known High Mass = 2.08+- 0.07 Msun

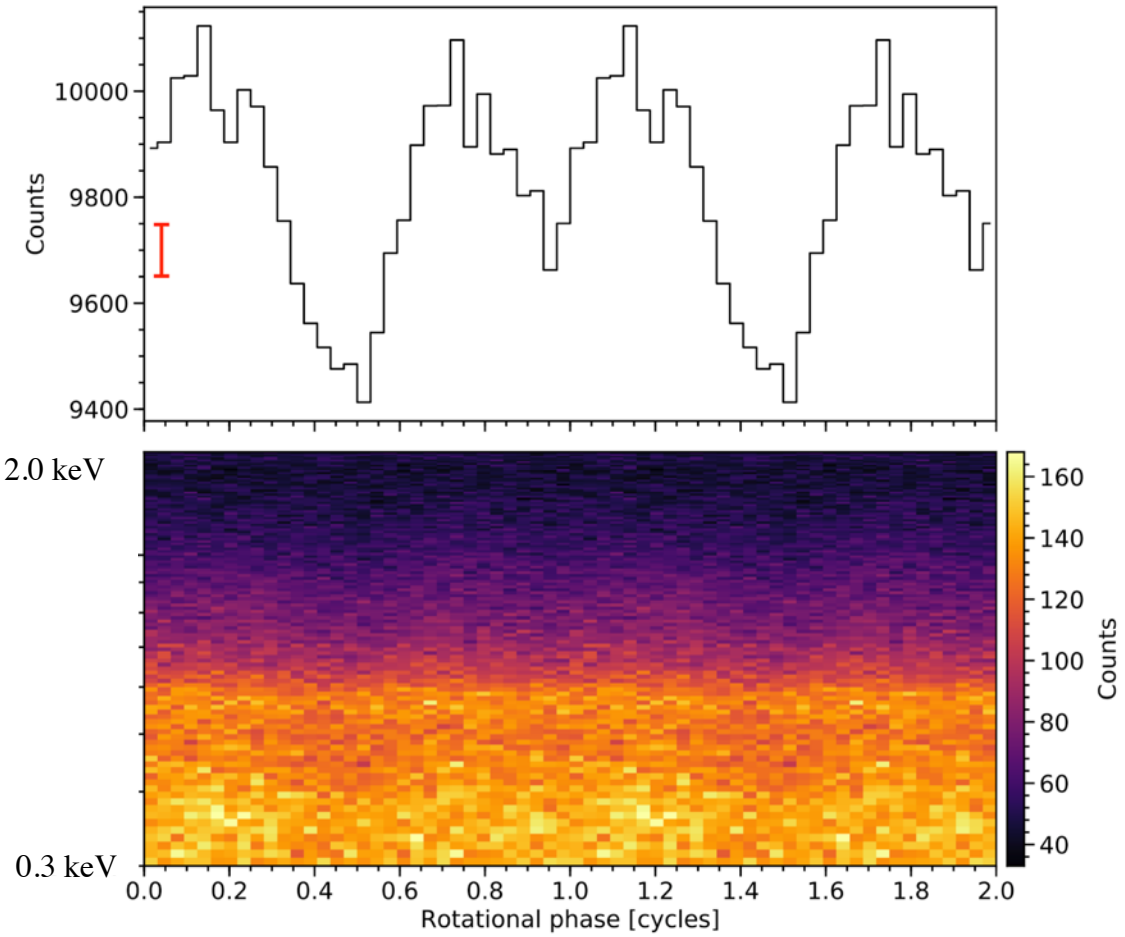

X-ray pulsations detected at 15 $\boldsymbol{\sigma}$ significance!

Wolff+ ApJL 2021

First Results on J0740

- Mass measurement from NANOGrav + CHIME:
  $M = 2.08 \pm 0.07\ M_{\odot}$ (Shapiro Delay, Fonseca+2021)
- Inclination close to 90 degrees (from radio obs)
- 2 Circular spots, closer to dipole than J0030
- Papers: Riley+ 2021, Miller+ 2021, Salmi+ 2022

Good agreement on 1 sigma lower limits (Salmi+2022)

$R_{1\sigma}$= 11.93 km (Amsterdam);

$R_{1\sigma}$= 11.98 km (Illinois-Maryland)

Next: J0437

- Closest pulsar! Great statistics!
- Precisely known value of mass and observer's viewing angle from radio observations
- Complication of contamination from background AGN in same field of view
- Results from J0437 and other pulsars in 2023/24

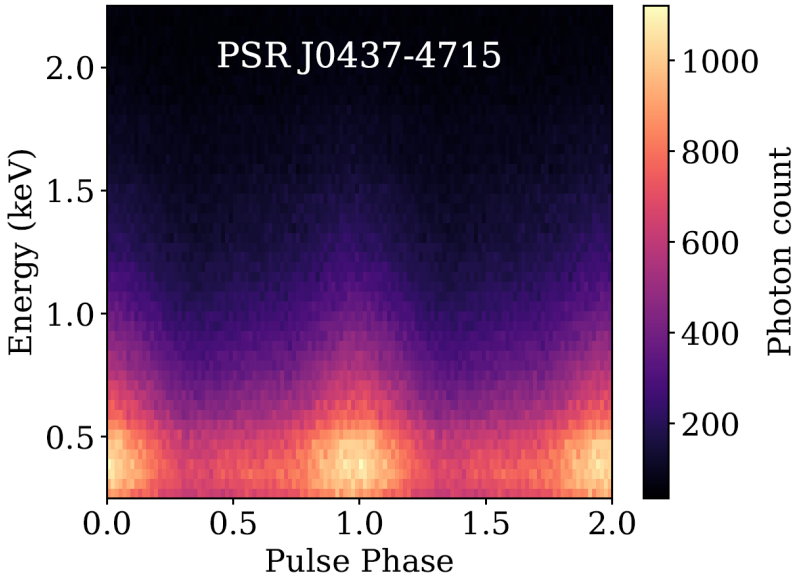

Cartoon of NICER 1-sigma constraints

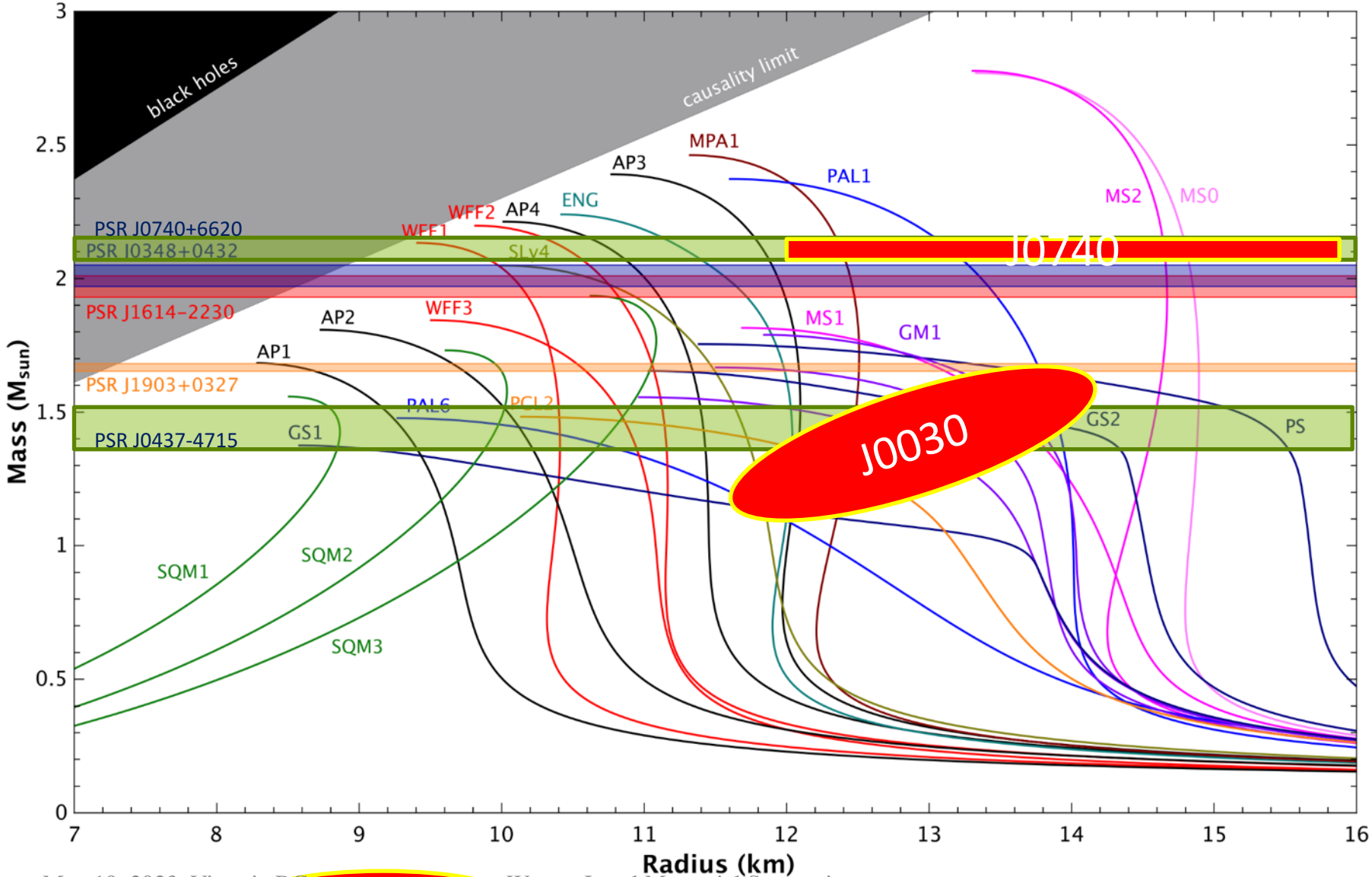

Credit: N. Wex

NICER Results on Core Science

- First precise measurement of mass through pulse-profile modelling (J0030)
- Radius inferred for 2 pulsars (J0030, J0740) with masses that differ by 0.5 M_{sun}
- Later this year
  - New results for J0437 (with precise radio prior for mass, inclination, distance)
  - Updated mass & radius results for J0030 & J0740 with improved precision

THE NICER LIGHTCURVE MODELING WORKING GROUP

Slavko Bogdanov (chair), Zaven Arzoumanian, Keith Gendreau, Anna Bilous, Deepto Chakrabarty, Devarshi Choudhury, Alexander Dittmann, Sebastien Guillot, Alice Harding, Wynn Ho, Fred Lamb, Jim Lattimer, Renee Ludlam, Simin Mahmoodifar, Cole Miller, Sharon Morsink, Chanda Prescod-Weinstein, Paul Ray, Ron Remillard, Thomas Riley, Tuomo Salmi, Tod Strohmayer, Serena Vinciguerra, Anna Watts, Michael Wolff, Kent Wood.

With thanks to Teru Enoto, Andrea Lommen, Matthew Kerr, Michi Bauböck, Feryal Özel, Craig Markwardt, Dimitrios Psaltis, Jack Steiner, & others

Summary

- We are in the golden era of NS observations!
- Amazing instruments today: LIGO/VIRGO/KAGRA, NICER, XMM, Chandra
- Bigger and better instruments planned for future both for Gravitational Radiation, and EM observations!
- Multiple methods for determining radius coming together with consistent values!